View metadata, citation and similar papers at core.ac.uk

brought to you by CORE

provided by Universidad Carlos III de Madrid e-Archivo

This is a postprint version of the published document at:

Sana, P. Vázquez, L., Cuerno, R. y Sarkar, S. (2017). Collective evolution of submicron hillocks during the early stages of anisotropic alkaline wet chemical etching of Si(1 0 0) surfaces. J*ournal of Physics D: Applied Physics*, 50(43).

DOI: https://doi.org/10.1088/1361-6463/aa87e8

© 2017 IOP Publishing Ltd.

Collective evolution of submicron hillocks during the early stages of anisotropic alkaline wet chemical etching of Si(100) surfaces

P. Sana[1], Luis Vázquez[2], Rodolfo Cuerno[3] & Subhendu Sarkar[1]

[1] Department of Physics, Indian Institute of Technology Ropar, Nangal Road, Rupnagar, Punjab, 140001, India

[2] Materials Science Factory, Instituto de Ciencia de Materiales de Madrid (CSIC), 28049 Madrid, Spain

[3] Departamento de Matemáticas and Grupo Interdisciplinar de Sistemas Complejos (GISC), Universidad Carlos III de Madrid, Avenida de la Universidad 30, 28911 Leganés, Spain

E-mail: sarkar@iitrpr.ac.in

Abstract. We address experimentally the large-scale dynamics of Si (100) surfaces during the initial stages of anisotropic wet (KOH) chemical etching, which are characterized through atomic force microscopy. These systems are known to lead to the formation of characteristic pyramids, or hillocks, of typical sizes in the nanometric/micrometer scales, thus with potential for the large number of applications that can benefit from nanotexturing of Si surfaces. The present pattern formation process is very strongly disordered in space. We assess the space correlations in such type of rough surfaces and elucidate the existence of a complex and rich morphological evolution, featuring at least three different regimes in just 10 minutes of etching. Such a complex time behavior cannot be consistently explained within a single formalism for dynamic scaling. The pyramidal structure reveals itself as the basic morphological motif of the surface throughout the dynamics. A detailed analysis of the surface slope distribution with etching time reveals that the texturing process induced by the KOH etching is rather gradual and progressive, which accounts for the dynamic complexity. The various stages of the morphological evolution can be accurately reproduced by computer-generated surfaces composed by uncorrelated pyramidal structures. To reach such an agreement, the key parameters are the average pyramid size, which increases with etching time, its distribution, and the surface coverage by the pyramidal structures.

1. Introduction

Texturing of silicon (Si) surfaces is important for several device fabrication processes which are advantageous for high speed capacitors, MOSFETs, high efficiency solar cells [1, 2, 3], CMOS [4], MEMS devices [5], optical switches [6], nanoprobes, laser cavities, etc. [7, 8, 9, 10, 11]. Anisotropic etching is a preferred texturing method owing to the presence of minimum defect densities/surface defects [12, 13] on the textured surface by changing the local etch rate [14, 15]. To reduce the time and production cost and to achieve high conversion efficiency without involving lithography, anisotropic texturing using alkaline hydroxide solutions such as potassium hydroxide (KOH), tetramethyl ammonium hydroxide (TMAH), etc. is a promising candidate as compared to other physical techniques [16, 5]. Wet etching of Si surfaces depends both on doping concentration and on the orientation of the surface [17]. Anisotropy is due to the fact that the removal of the surface atoms is a site-dependent process at the microscopic scale [18]. The etch anisotropy ratio for Si in the (111):(110):(100) directions is approximately 1:600:400 [19]. The formation of pyramidal structures, or hillocks, on the Si (100) surface is a result of the high etch rate of (100) and (110) planes in comparison with the (111) planes, leading to slower etching of the latter [20, 21]. Although it is now agreed that the hillocks nucleate thanks to some mechanism that stabilizes their apices, the precise nature of the mechanism remains to be understood [22, 18, 23, 24]. Elwenspoek [25] has shown that the slowest etch rate of (111) surfaces is primarily due to their higher step free energy which increases the activation energy for cavity formation process during the KOH etch. Later, a theoretical study indicated that the microscopic activation energy of the surface atoms for a particular plane is determined by the nearest and next-nearest atoms and the plane symmetry [19]. Other studies have established a realistic connection between the macroscopic activation energy of the etch rate and the microscopic activation energies of the atomistic processes [26, 27].

From a general point of view, owing to the miniaturization of devices, in recent years the improved understanding of the roughness of the etched surface has gained importance both, from the practical and from the fundamental points of view. It has thus become important to determine precise fabrication conditions for these structures that lead to desired levels of surface smoothness. The topographical changes that take place during Si wet etching have already been studied in this context, both experimentally and theoretically [28, 29, 30]. These works also address pyramidal hillock formation on Si surfaces, which constitutes a major source of roughness along the time evolution of the system. Actually, under conditions in which large fluctuations take place in the statistics of the morphology [31], the study of the collective properties of the surface frequently allows to infer the type of physical mechanisms which drive the topographical behavior [32, 33]. This type of approach has been successfully employed to understand surface physical or chemical growth or erosion mechanisms governing topography for a number of systems [34, 35, 36, 37, 38, 7, 39, 40, 41]. For the specific case of Si etching, quantitative studies in this direction have also been performed

[35, 42, 21, 43]. Thus, for experimental NaOH etching [35], percolation properties have been assessed for the ensuing in-plane arrangement of mound-like hillocks, whose out-of-plane correlations display so-called anomalous scaling [44, 45, 46]. Isotropic Si etching has been studied experimentally [42] and compared qualitatively with kinetic Monte Carlo (kMC) simulations of one-dimensional models [21]. More recently [43], some properties of the average surface roughness have been assessed experimentally for KOH anisotropic etching, including dependence with temperature. In particular, it has been determined that the surface roughness increases initially with etching time, to finally reach a saturation or steady-state [47, 14, 48]. The dynamics of hillocks in this regime has been studied experimentally and modeled using the Monte Carlo method by allowing for site-dependent detachment probabilities [48].

In this paper, we address the intial stages of surface etching (up to 10 minutes of etching under our working conditions, see below), in which the surface roughness increases with time, that is, well before roughness saturation. We study the dynamical evolution of the submicrometric hillock pattern that ensues under anisotropic KOH etching of Si(100) surfaces, focusing on the collective morphological properties of the surface, as well as their behavior with etching time. Although strongly disordered, the surface morphology is not uncorrelated. Actually, it features space correlations with scale-invariant properties akin to those found in kinetically rough systems, which in principle indicates non-trivial behavior in the spatial self-organization of the hillock pattern [31, 32, 33, 49, 50]. In particular, conspicuously large fluctuations are found to take place in the values of the surface height from point to point on the substrate. However, the time evolution is more complex than in other experimental instances in which rough interfaces occur, to such an extent that the morphological behavior is hard to reconcile with the precise expectations for kinetically rough surfaces [31, 49, 50]. This suggests the existence of very different mechanisms controlling the collective behavior of the hillock pattern at different stages during the time evolution, a fact which is also supported by the observed time evolution of the statistical distribution of the facet angles, which evidences a gradual texturization process. Notwithstanding, systematic comparison of our experimental hillock arrangements with those synthetically obtained through open software [51] allows us to interpret the geometrical content of the space correlation functions which we measure. These findings are discussed in the light of the different physical mechanisms proposed for hillock formation and dynamics under wet chemical etching of Si(100) surfaces.

2. Experiment

2.1. Sample preparation

Undoped single-side polished Si (100) surfaces were chemically etched using a KOH solution in a clean room environment. The Si wafers were procured from Vin Karola Instruments grown by Czochralski method and having an electrical resistivity

$\simeq 15 - 20\ \Omega$-cm. Samples were prepared for different etch times. 1×1 cm^2 Si wafers, cut from 2 inch-diameter wafers, were ultrasonically cleaned for 15 minutes at room temperature with isopropyl alcohol. Each wafer was rinsed with ultrapure deionized water after sonication using a Millipore system. A 7 wt% (1.25 M) KOH solution was taken and kept on stirring at a constant temperature of 80° C for 1.5 hours. According to the literature, these can be considered as low concentration conditions. The Si wafer was dipped into KOH solution for a specific etch time at room temperature which was kept constant for the entire process. Identical procedure was employed to etch Si wafers for etch times of 30, 90, 120, 240, 360, 480, and 600 seconds.

2.2. Sample characterization

The surface morphologies of the etched Si wafers were measured using Bruker Multimode-8 Atomic Force Microscopy (AFM) in tapping mode. For each sample, 512×512 pixels images were acquired for three different image lateral sizes of 10, 25, and 50 microns. For each scan size, three different regions were scanned to account for better statistics and data reproducibility. Silicon cantilevers (Bruker) with a nominal radius of 8 nm were employed.

3. Results

3.1. Morphological characterization and scaling analysis of as-prepared samples

AFM images of KOH etched Si surfaces for different etch times are shown in Fig. 1. Transverse one-dimensional cuts of these images are additionally shown in Fig. 2. After an etching time of 30 s, mounded structures appear scattered on the Si surface. These structures grow in size between 90 and 120 s, leading to a rather high density of bright spots which is highest at 120 s, when the protruding structures become 500-700 nm wide. As can be seen in the inset, some of these structures already have a faceted pyramidal morphology, while others are more rounded. However, at 240 s this process has led to the emergence of a few, well-defined pyramidal structures, with a bright contrast and a rather heterogeneous size distribution. These are surrounded by smaller structures, see inset. With further etching, pyramids grow and display sharper forms. At an etch time of about 480 s, these pyramids practically form a homogeneous and compact surface. Finally, large hillocks are observed after etching the sample for 600 s, akin to the 240 s case, but with a higher pyramid coverage. Figures 1 and 2 indicate the existence of two basic lateral lengths in the morphologies, namely, the motif size, ξ, and the average inter-motif distance, λ. They are evident in the corresponding profiles for 240 s, 360 s, and 600 s, where large protruding pyramidal structures are visible that are not compactly arranged. For other etching times, there is also a distribution of structures, most of which resemble a basic motif, a square pyramid. These structures are quite disordered on the substrate plane within a single AFM image, leading to a wide distribution of the inter-pyramid distances.

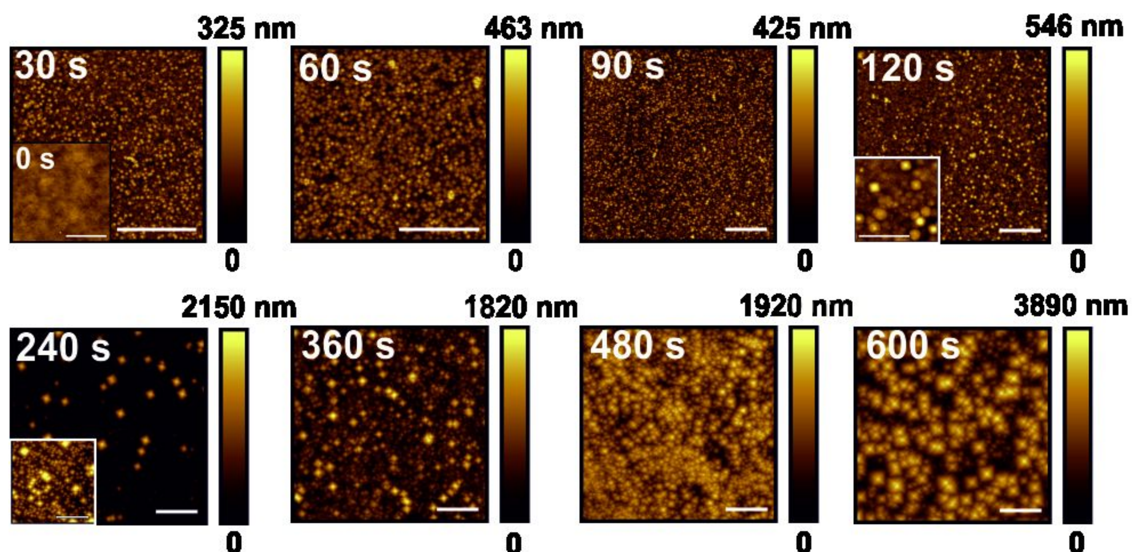

Figure 1. AFM top-views of the Si(100) surfaces for etching times as provided in the legends. Height color bars are provided on the right of each top view; the differences in scales between different images reflect roughness increase with time. The inset in the 30 s image corresponds to the initial pristine Si surface (0 s). The scale bars represent 10 μm. The insets for 120 s and 240 s show higher resolution images taken on the corresponding backgrounds. The scale bars represent 3 μm.

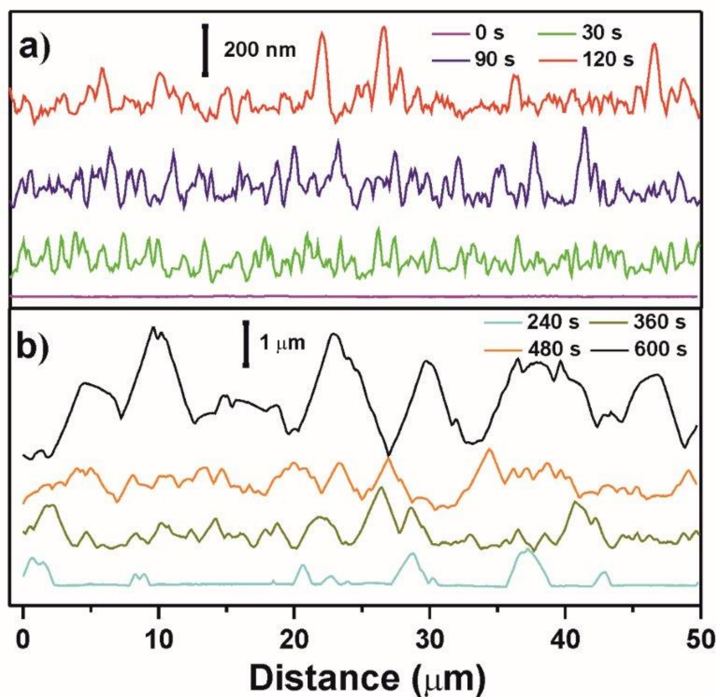

Figure 2. Typical surface profiles for the etched surfaces for times: (a) from 0 to 120 s, and (b) between 240 and 600 s. Solid bars provide the vertical scales in each case and differ by a factor of 5 between the two panels.

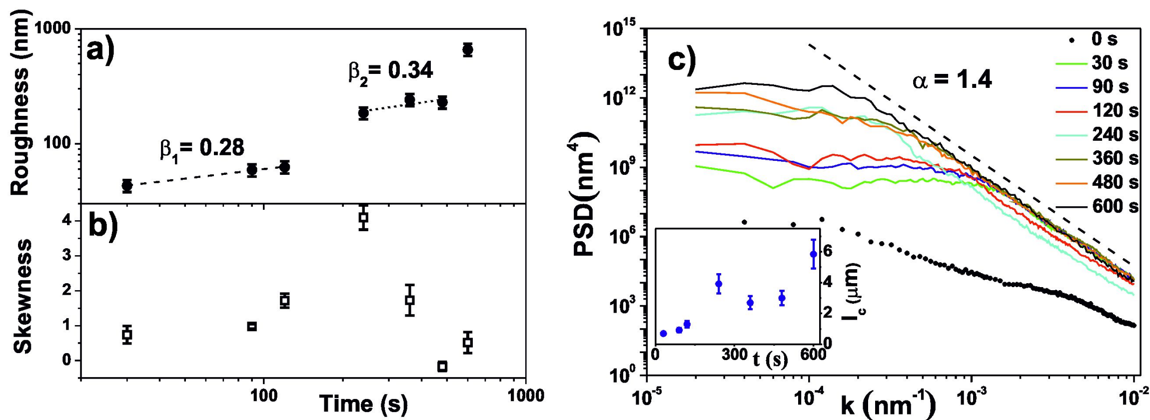

Figure 3. (a) Log-log plot of the experimental global surface roughness W vs etching time. For reference, the straight lines correspond to power-law behavior $W \sim t^{\beta}$ with values for β as indicated.(b) Plot of the experimental surface skewness γ_1 vs etching time. (c) Log-log plot of the (radially-averaged) experimental PSD for etching times as indicated in the legend. The bullets correspond to the pristine Si(100) surface. For reference, the dashed straight line represents the power-law behavior $S(k) \sim 1/k^{2\alpha+2}$ with $\alpha = 1.4$. Inset: Plot of the correlation length l_c obtained from the corresponding PSD curves (see text) as a function of etching time.

Overall, the AFM images show large-scale surface roughening and faceting. In order to have deeper insight into the surface dynamics, we have analyzed the evolution of the global surface roughness, $W(t)$ [31, 49], with etching time t, provided in Fig. 3a. For each time, $W(t)$ has been computed using those images that have the largest lateral size, $L = 50$ μm. Indeed, the global roughness increases with time at changing rates that last short periods of roughly 2 to 4 minutes. Thus, the initial stages when mound structures emerge are characterized by a relatively slow roughening, $W(t) \sim t^{\beta_1}$ with a value of the growth exponent $\beta_1 = 0.28$. Moreover, the change in the growth regime at 240 s suggested by the AFM image in Fig. 1 is confirmed by the sharp increase in the value of the roughness: indeed, $W(t = 240$ s) is more than three times larger than $W(t = 120$ s). However, the roughening process slows down between 240 s and 480 s, so that $W(t) \sim t^{\beta_2}$ with $\beta_2 = 0.34$. This regime corresponds to the gradual increase of the hillock density that finally reaches full coverage by pyramids at 480 s, similar to the behavior between 30 s and 120 s. Finally, at 600 s the roughness increases again substantially, becoming more than twice its value at 480 s.

Another statistical parameter that is helpful to describe the interface morphology is the skewness, $\gamma_1(t)$, that measures the lack of up-down symmetry of the distribution of height values around its mean [49]. The experimental time evolution of γ_1 is plotted in Fig. 3b. Thus, from 30 s to 120 s the skewness increases from 0.4 to 1.5. At 240 s, γ_1 undergoes a huge increase up to a value larger than 4, which correlates with the emergence of a few, large pyramids from the background. Afterwards, between 360 s and 480 s, the skewness goes back to values which are similar to those measured within the initial time regime, with a minimum at 480 s, i.e., when the surface is fully covered

by the pyramid structures. Finally, at 600 s γ_1 increases again due to the fact that the surface is not fully covered by the large pyramids. Summarizing, the behavior of the skewness seems to correlate with the surface coverage by the emerging pyramids with respect to the homogeneous background, and to the average pyramid height relative to the surface roughness. Large γ_1 values are obtained when this coverage is low and the pyramids are relatively high, whereas the skewness is reduced for a surface with a high density of hillocks, particularly when the pyramid coverage tends to unity, due to the enhanced symmetry of the surface morphology with respect to its average height.

Qualitatively, the behavior observed for the global roughness and the skewness suggests the following surface evolution: 1) slow roughening and an increase of γ_1 (associated with the emergence of mounds) up to 120 s. 2) A sharp increase of W associated with the development of few large pyramids at 240 s, leading to a substantial increase of the skewness. 3) Slow-down of the roughening process between 300 and 480 s, due to the gradual covering of the surface by the emerging pyramids, which become more numerous with time, decreasing the value of γ_1. 4) At 600 s, W increases again due to the incomplete coverage of the surface by the existing pyramids. Similar patterns are frequently observed at long times in the present type of wet etching process [47, 48, 43].

Both, roughness and skewness are *global average* quantities that characterize the behavior of the surface as a whole. Further detailed information can be gained from a study of correlation functions, which are sensitive to the morphological behavior at different scales. A very useful one [32] is the surface structure factor or power spectral density (PSD) [31, 49] $S(k,t)$, where k is the wave-vector magnitude. Figure 3c shows the (radially-averaged) PSD function obtained for different etching times including the pristine initial Si(100) surface. Note how the initial space correlations, encoded in the dependence of $S(k,t)$ with k, have disappeared at all length-scales (equivalently, all values of wave-vector k) already after 30 s etching time. For each time, the behavior of the PSD can be roughly seen to feature a k-independent (-dependent) behavior for small (large) wave-vectors. The former implies that parts of the surface remain statistically independent, i.e., uncorrelated, at the corresponding large distances. The latter behavior is approximately consistent with power-law decay in the form $S(k) \sim 1/k^{2\alpha+2}$ for a suitable choice of the so-called roughness exponent α. For any fixed time, there is a wave vector value k_c separating small-k from large-k behaviors in the PSD. We estimate it (with up to 20% error bars) by measuring the crossing point between the straight line defined by the linear dependence observed at large k (parallel to the dashed line in Fig. 3c) and a horizontal line describing uncorrelated, k-independent behavior.‡ The inverse of this characteristic wave-vector defines the correlation length, $l_c = 1/k_c$, i.e. a lateral distance within which height values are statistically correlated variables. The inset of Fig. 3c shows the thus obtained values of l_c for different times. The correlation length increases from 700 nm at 30 s up to almost 4 μm at 240 s, then decreases down to 2.5-3 μm in the 360-480 s range, and increases back up to 5.8 μm at 600 s.

‡ Statistically relevant length scales can be equivalently obtained from the time behavior of the surface roughness $w(l,t)$, as obtained over images of lateral size l, see Fig. S1 in Suplemental Material.

The existence of a basic motif (the square pyramids) in our experimental topographies suggests the relevance of two associated scales, namely, the average pyramid size ξ and the average inter-pyramid distance λ, which should be identifiable e.g. in the PSD data, akin to island formation in submonolayer growth [52] and to mound formation in multilayer growth [50]. Indeed, e.g. in the former context λ can be identified from the occurrence of a well-defined maximum in the PSD at relatively small k. However, the k-dependence of our PSD curves is less clear-cut for small k and requires a more detailed study, performed in Sec. 3.2 below.

For now, we focus on the experimental large-k behavior, corresponding to distances smaller than the average pyramid size. As seen in Fig. 3c, the power-law behavior that is obtained is well characterized by $\alpha = 1.4 > 1$, the PSD for different times overlapping except for 120 and 240 s. This behavior is reminiscent of so-called kinetic roughening [31, 49]. A surface is said to be kinetically rough if its time and space correlations follow power laws like $W(t) \sim t^{\beta}$ or $S(k) \sim 1/k^{2\alpha+2}$, where α and β are related in a precise way. This is encoded in a so-called dynamic scaling Ansatz for the space and time behavior of correlation functions [31, 49], which generalizes to non-equilibrium systems (hence the name kinetic) the classic scaling Ansatz describing equilibrium critical phenomena or second-order phase transitions [53]. However, power-law correlations can also occur for surfaces whose topography is dominated by a characteristic form or motif [54, 55, 56] and which are not kinetically rough because the expected scaling Ansatz is not fulfilled. We believe this is the case in our experiments, in contrast with previous works that discuss similar wet etching processes in the kinetic roughening context [35, 42, 21, 43]. Namely, attempts to consistently analyze our data under the most comprehensive formulation of the dynamic scaling Ansatz compatible with our result that $\alpha > 1$ [45] prove unsuccesful. Hence, we believe that the exponent α that we measure originates in the well-defined geometry of the pyramids rather than in kinetic roughening.

3.2. Synthetic patterns

In order to assess the morphological relevance of the pyramidal motif along the full etching process, it is useful to analyze the slope distribution of the images. This is done in Fig. 4a (left column), which shows the AFM images of the surfaces etched after 90 and 600 s, with the corresponding slope histograms as insets. Specifically, the slope distribution shown is a 2D plot in which the independent variables are the space derivatives of the height, $m_x = \partial h/\partial x$ and $m_y = \partial h/\partial y$ along the two coordinate direction on the AFM images; the dependent variable is the fraction of points of the original AFM topograph at which the slopes happen to equal the pair of values (m_x, m_y). Indeed, the two experimental surfaces display a square-symmetric pattern, as evidenced by the form of the corresponding slope histograms. This is more clear for the 600 s image, for which the signal is particularly enhanced at the vertices. In contrast, for the 90 s surface the square pattern is more blurred, although still discernible. Therefore, the slope distribution suggests that a similar basic motif is the basic component of the

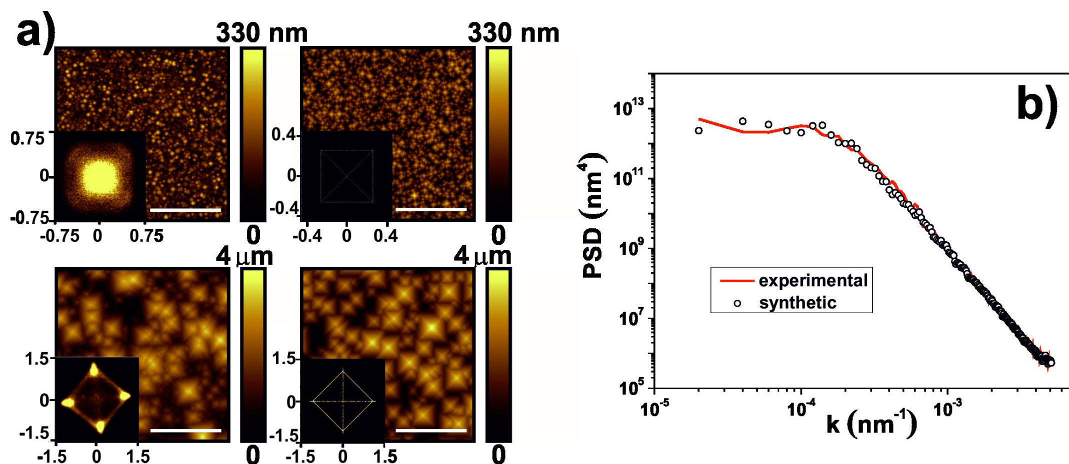

Figure 4. (Panel a): Left column: experimental AFM images of silicon surfaces etched for 90 s (top) and 600 s (bottom). Right column: Synthetic random arrangements of square pyramids resulting in images of similar roughness as the corresponding experimental image shown on the same row. All horizontal size bars represent 10 μm. Insets: 2D slope histograms. (Panel b): Radial PSD functions of the experimental AFM image (solid line) and of the synthetic surface (open symbols), both corresponding to a scan size of 50 μm for an etch time of 600 s.

morphology already from the very early stages of the process, namely, the square hillocks that are so evident in the AFM topograph at 600 s. For the shortest etching times the slope distribution is more diffuse, indicative of an incipient surface texturing process.

The fact that the basic structural motif of the evolving surface is pyramidal allows us to model the surface at the different stages by producing synthetic surfaces that readily employ such a basic morphological unit. Specifically, we make use of Gwyddion [51], an open software package for surface data analysis, in order to generate random arrangements of square pyramids. For each etching time, we have tuned the parameters controlling the synthetic surface in order to reproduce, not only the measured surface roughness, but also the full experimental PSD curve, thereby reproducing the space correlations experimentally measured at that time. In this process, we have found that there are two key parameters [see the Supplementary Information (SI) for further details]: the *first* and most important one is the average size of the pyramids. Thus, in order to accurately reproduce the experimental surface correlations, we have increased the pyramid size with etching time (using motif size/image size ratios of 0.5%, 0.9%, 1.2%, 2%, 2.3%, 2.9%, and 4.5% for increasing times). Simultaneously, we have kept fixed the variance of the distribution of pyramid sizes to a relatively low value, 0.21, for all etching times. The *second* main parameter that controls agreement between experimental and synthetic surfaces is the coverage of the surface by the randomly arranged pyramids. We define pyramid coverage [51] as the average number of pyramids which cover a pixel on the image. Hence, for synthetic surfaces in which the pyramids visually fill the whole surface with coverage larger than 1, there is substantial overlapping of different pyramids. Specifically, we have employed pyramid coverage equal to 4, except

for 30 s (coverage = 0.8) and 240 s (coverage = 0.32).

In this way, by changing the average pyramid size and by re-scaling the lateral and vertical dimensions, we are able to reproduce the experimental images, not only qualitatively but also quantitatively. Qualitative agreement can be appreciated in Fig. 4a (right column), which shows the synthetic images for 90 s (top) and 600 s (bottom), in parallel with the corresponding experimental AFM top views. The visual similarity between the experimental and synthetic images is striking, specially for 600 s. The 2D slope distributions of the synthetic morphologies are also shown as insets. The clear square-symmetric patterns confirm our previous conclusions with respect to the experimental images. The increased sharpness of the pattern in the synthetic surface for the short etching time indicates that, at the beginning of the process, the pyramidal structures are not so well developed yet. Indeed, the contrast of the 2D slope distributions is sharper and more homogeneous along the square sides in the synthetic cases, as expected due to the perfection of their pyramidal motifs. Quantitative agreement between the experimental and synthetic surfaces is confirmed in Fig. 4b, where we show the PSD functions of the experimental and the synthetic 50×50 μm^2 images, for 600 s etching time. Note that the two sets of data match throughout k-space, implying virtually identical values of the global roughness. This type of quantitative agreement has been reproduced for all the etching times and scan sizes by suitably tuning the motif size, with the exceptions noted above. Small discrepancies have only been found at large k-values for the smallest images carrying a smaller number of individual hillocks, where some aliasing effects also take place.

The possibility to match the experimental images with synthetic surfaces composed by randomly arranged pyramids allows us to better interpret the PSDs of Fig. 3c. As noted above, two basic length scales should occur in this system, ξ and λ. Whereas the former is related to the power-law regime for large k, the latter should appear as a peak in the PSD for lower k values [52, 50], which is not clearly seen in Fig. 3. In the SI we further analyze our synthetic surfaces for different parameter values of the random pyramid distribution. The conclusion is that large pyramid sizes relative to the image size and large surface coverage by pyramids hamper the occurrence of the peak in the PSD which is associated with the inter-pyramid distance λ. Morphological analysis like that in [52] for submonolayer pentacene islands on flat silicon oxide surfaces can allow to identify ξ and λ in the PSD. However, this is only possible when the surface coverage by pyramids is relatively small, which in our case occurs up to 240 s, see the SI. The high coverage and disorder of our experimental pyramid distribution for longer times hampers application of the approach in [52]. Nevertheless, the value of λ and ξ can still be inferred from the Autocorrelation (ACF) and height different correlation (HDCF) functions [50], see the SI. Indeed, the two distances are closely correlated for $t < 240$ s, as expected for an arrangement of well-defined pyramids, while they are not clearly related for longer etching times, supporting a more random positioning of pyramids.

4. Discussion

The results obtained in the previous sections suggest that: (i) non-trivial space correlations build up in the surface patterns, (ii) at an etching time of approximately 240 s there is a change of behavior in the system; (iii) two basic lengths exist in the morphologies, namely, the pyramid size and the inter-pyramid distance, particularly for long etching times. The surface morphology does not display kinetic roughening properties [31], power-law behavior at distances smaller than the pyramid size being induced by the geometry of this basic motif.

The quantitative description of the experimental space correlations by our synthetic surfaces allows us to think of the morphologies in terms of a random distribution of pyramids. We can further consider this fact in the light of the scenario of wet etching of silicon surfaces reviewed in the Introduction. Thus, the etching process becomes inhibited at some locations (through some of the various mechanisms proposed) that become apices wherefrom growth of pyramidal hillocks nucleates. Depending on the specific mechanism that operates, these nucleation sites can change or lose their condition dynamically, leading to a complex morphological evolution. A scenario like this corresponds in general terms to an etching process with poisoning [57]: indeed, the large surface fluctuations implied by the fact that $\alpha = 1.4 > 1$ (and the time behavior of the roughess, as assessed in the SI) agree with this behaviour. This is consistent with the view that wet etching of Si(100) proceeds via etching inhibition at certain sites, already at the early stages of the process.

We can obtain further insight into the present rich morphological dynamics by considering further experimental properties of the hillock assembly. As mentioned above, one of the main mechanisms leading to the pyramidal texturization of the Si(100) surface is based on the slower etching rate of the $\{111\}$ planes. Hence, it is natural to study the time evolution of the facet angles with respect to the flat Si(100) plane. The corresponding data are displayed in Fig. 5, where we show the distribution (histogram) of facet azimuth angles for different etching times. We consider the azimuth to be the angle subtended by the projection of the normal direction to the facet onto the xy substrate plane with the x axis; it measures the facet orientation. Initially, up to 120 s a bimodal distribution is observed with predominant angles around 10° and 30°. This corresponds to the emergence of mounded structures. After 240 s this distribution is even narrower and less symmetric, with a preferred maximum close to 5° (due to the smoother background) and a secondary maximum near 50° (due to the large pyramids). This correlates with the clear observation of scattered, large, and well-formed pyramidal structures on the surface. At later times, a higher slope, close to 50°, develops, which becomes predominant after 600 s of etching. We should remark that the ideal angle between the $\{111\}$ and $\{100\}$ planes is 54.7° [24], very close to this value. Hence, the present data indicate a texturization process which evolves rapidly with time. The different dynamical stages detected in the dynamics of the roughness are related to the progressive faceting of the surface, whereby close-to-perfect pyramids eventually form.

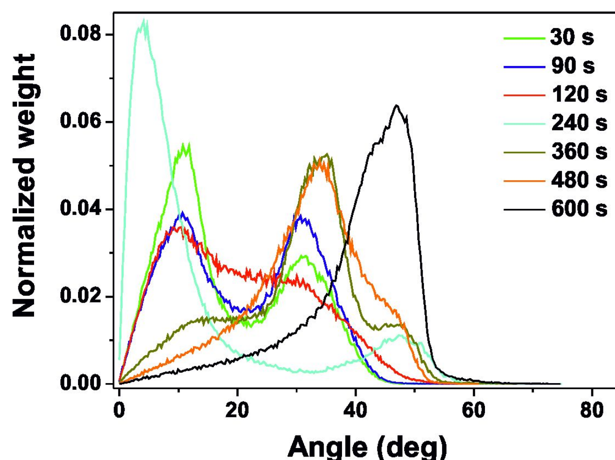

Figure 5. Normalized facet azimuth angle distribution for the experimental surfaces at different etching times, as indicated in the legend.

Note also that, as {111} planes are becoming more populated, i.e. with progressive texturization, the average etching rate decreases. Interestingly, for etching times longer than 240 s the faceting process continues mainly via formation of smaller pyramid structures, rather than through the coarsening and growth of existing ones, see Fig. 2. This is consistent with the relatively low KOH concentration condition employed in our studies. Under these conditions, the etching of the background (non texturized) surface is relatively slow, which allows the formation of new pyramidal structures before the existing ones grow in height and size. This is also consistent with the fact that at 600 s the surface is basically composed by a distribution of pyramidal structures with a small dispersion of sizes. Recall that, in the synthetic patterns, a low variance value of the motif size was used.

We still need to address in further detail how the observed morphological behavior can be understood under the framework of the poisoning mechanisms mentioned in the Introduction. These mechanisms include the effect of bubbles [14], the adsorption of inhibiting species, like metals, from the solution [22], and the selective reactivity of specific sites on the surface [58, 24]. The effect of bubbles on the morphology is supported by the observation that, under stirring conditions which specifically prevent bubble formation, the hillock density and size are largely reduced [22]. The two remaining mechanisms are based on processes that take place at atomic scales. For instance, detailed numerical simulations are available in the literature [22, 18, 48], in which the formation and evolution of the pyramidal structures during wet etching of Si(100) surfaces is addressed. A main goal of these studies is to assess the specific microscopic mechanism that controls the onset of pyramid formation. However, it may be hard to directly infer from microscopic models the collective behavior of the surface morphology composed by an assembly of pyramids, such as is our present focus.

Under the experimental conditions that we study, masking of surface sites through the formation of hydrogen bubbles seems unlikely. First, the relatively low KOH

concentration conditions should induce formation of relatively large, or at least medium-sized, bubbles [14] that, accordingly, would lead to large pyramid sizes, which is not the case in the initial stages that we address. Moreover, except for the 240 s case, our surfaces are quite homogeneous, which suggests a uniform distribution of small bubbles over the surface. This scenario seems unlikely at these KOH concentration and short etching times. The additional mechanisms of inhibitor species [22] or selective site reactivity [58, 24] are based on a slower or null etching rate at given surface sites which thus become the pyramid apices. The latter mechanism was proposed for a H-terminated Si surface, which is likely not the case for our system due to the KOH etching, which induces the formation of OH-terminated sites on the Si surface [59, 14]. In the former mechanism, the pyramid apices would be a consequence of the presence of species that inhibit etching. When they arrive to the surface from the solution, they should do so along random trajectories, in such a way that they would impinge the most exposed surface locations with a higher probability. In that case they would inhibit surface sites randomly. Upon stirring, the arrival of these species should be more homogenously distributed on the surface, which might be related with the reduced pyramidal structuring.

5. Conclusions

In summary, we have studied the early-time regime of nano-pyramid hillock formation under alkaline wet chemical etching of silicon targets. Overall, the process can be understood in terms of the formation of mounds that evolve into characteristic and well-formed square pyramids, emergence of individual pyramids being essentially uncorrelated in space. Two basic length scales characterize the surface morphology, namely, the pyramid size and the average inter-pyramid distance. The non-trivial behavior of experimental space correlation functions can be attributed to the occurrence of a well-defined pyramidal shape, coexisting with a strong heterogeneity. The behavior of correlations with etching time does not agree with kinetic roughening properties, likely due to the gradual surface texturing process that is taking place.

At any fixed time the full behavior of the observed space correlation functions can be quantitatively reproduced by that of synthetic images that have been obtained employing freely available software for surface data analysis. Actually, this agreement validates the representation of the process in terms of the uncorrelated emergence of individual, well-defined pyramids. On the way, the variation of the correlation functions of the synthetic interfaces with parameters underscores the dynamical relevance of the average pyramid size and of the surface coverage by pyramids as the main experimental features determining the morphological properties of the experimental surfaces. Finally, our findings seem to agree, at least partially, with physical mechanisms for hillock formation under wet etching which are based on some type of poisoning, more than with those advocating alternative processes, such as bubble formation.

Acknowledgments

We gratefully acknowledge discussions with David Nečas, leader of the Gwyddion project. This work was supported by Council of Scientific and Industrial Research (India) Scheme No. 03(1289)/13/EMR-II, and by MINECO/FEDER (Spain/UE) Grants Nos. FIS2012-38866-C05-01, MAT2014-54231-C4-1-P, BIO2016-79618-R, and FIS2015-66020-C2-1-P, as well as by Comunidad Autónoma de Madrid (Spain) Grant NANOAVANSENS S2013/MIT-3029.

References

[1] Silva A R, Miyoshi J, Diniz J A, Doi I and Godoy J 2014 *Ener. Proc.* **44** 132–137
[2] Wang F, Zhang X, Wang L, Jiang Y, Wei C and Zhao Y 2015 *J. Power Sources* 698–705
[3] McIntosha K R and Johnson L P 2009 *J. Appl. Phys.* **105** 124520
[4] Lee M, Jeon Y, Moon T and Kim T 2011 *ACS Nano* **5 (4)** 2629–2636
[5] Pal P, Sato K and Chandra S 2007 *J. Micromech. Microeng.* **17** R111–R133
[6] Yang Y J and Liao B T 2009 *IEEE Photonics Technol. Lett.* **21** 2
[7] Dimitrov D Z and Du C H 2013 *Appl. Surf. Sci.* **266** 1–4
[8] Xiu F, Lin H, Fang M, Dong G, Yip S and Ho J C 2014 *Pure Appl. Chem.* **86(5)** 557–573
[9] Fesquet L, Olibet S, Damon-Lacoste J, Wolf S D, Hessler-Wyser A, Monachon C and Ballif C 2009 Modification of textured silicon wafer surface morphology for fabrication of heterojunction solar cell with open circuit voltage over 700 mv *Photovoltaic Specialists Conference (PVSC), 2009 34th IEEE* pp 000754–000758 ISSN 0160-8371
[10] Sridharan S, Bhat N and Bhat K N 2013 *Appl. Phys. Lett.* **102** 021604
[11] Khanna A, Basu P K, Filipovic A, Shanmugama V, Schmiga C, Aberle A G and Mueller T 2015 *Sol. Energy Mater. Sol. Cells* **132** 589–596
[12] Adriana E L and John E S J 1999 *J. Appl. Phys.* **85** 876
[13] Kulkarni M S 2003 *Ind. Eng. Chem. Res.* **42 (12)** 2558–2588
[14] Haiss W, Raisch P, Bitsch L, Nichols R J, Xia X, Kelly J J and Schiffrin D J 2006 *J. Electroanal. Chem.* **597** 1–12
[15] Zhuang D and Edgar J 2005 *Materials Science and Engineering: R: Reports* **48** 1 – 46 ISSN 0927-796X
[16] Kim J, Inns D, Fogel K and Sadana D K 2010 *Sol. Energy Mater. Sol. Cells* **94**(12) 2091–2093
[17] Seidel H, Csepregi L, Heuberger A and Baumgartel H 1990 *J. Electrochem. Soc.* **137**(11) 3612–3626
[18] Gosálvez M A, Sato K, Foster A S, Nieminen R M and Tanaka H 2007 *J. Micromech. Microeng.* **17** S1–S26
[19] Jiang Y and Huang Q A 2005 *Semicond. Sci. Technol.* **20** 6
[20] Bassous E 1975 *IEEE Transac. Electron Dev.* **ED 25** 10
[21] Mirabella D A, Suarez G P, Suarez M and Aldao C M 2014 *Physica A* **395** 105–111
[22] Gosálvez M A and Nieminen R M 2003 *New J. Phys.* **5** 100.1–100.28
[23] Montesdeoca-Santana A, Orive A G, Creus A H, González-Díaz B, Borchert D and Guerrero-Lemus R 2013 *Micros. Microanal.* **19** 285–292
[24] Skibinski E S and Hines M A 2015 *J. Phys. Chem. C* **119** 14490–14498
[25] Elwenspoek M K 1993 *J. Electrochem. Soc.* **140(7)** 2075–2080
[26] Gosálvez M A and Nieminen R M 2003 *Phys. Rev. E* **68**(3) 031604
[27] Gosálvez M, Cheng D, Nieminen R M and Sato K 2006 *New J. Phys.* **8** 269
[28] Veenendaal E V, Sato K, Shikida M and Suchtelen J V 2001 *Sens. Actuat. A: Phys.* **93**(3) 219–231
[29] Yang C R, Yang C H and Chen P Y 2005 *J. Micromech. Microeng.* **15** 11
[30] Pal P and Sato K 2015 *Micro and Nano Systems Lett.* **3:4** 1–42

[31] Barabási A L and Stanley H E 1995 *Fractal Concepts in Surface Growth* (Cambridge: Cambridge University Press)
[32] Cuerno R and Vázquez L 2004 Universality issues in surface kinetic roughening of thin solid films *in Advances in Condensed Matter and Statistical Physics* ed Korutcheva E and Cuerno R (New York: Nova Science Publishers) p 237
[33] Cuerno R, Castro M, Muñoz-García J, Gago R and Vázquez L 2007 *Eur. Phys. J. Special Topics* **146** 427–441
[34] Ojeda F, Cuerno R, Salvarezza R and Vázquez L 2000 *Phys. Rev. Lett.* **84** 3125
[35] Dotto M E Rand Kleinke M U 2002 *Phys. Rev. B* **65** 245323
[36] Auger M A, Vázquez L, Cuerno R, Castro M, Jergel M and Sanchez O 2006 *Phys. Rev. B* **73** 045436
[37] Takeuchi K A, Sano M, Sasamoto T and Spohn H 2011 *Sci. Rep.* **1** 1
[38] Yang J J, Tang J, Liu N, Ma F, Tang W and Xu K W 2012 *J. Appl. Phys.* **111** 104303
[39] Yunker P J, Lohr M A, Still T, Borodin A, Durian D J and Yodh A G 2013 *Phys. Rev. Lett.* **110** 035501
[40] Nicoli M, Cuerno R and Castro M 2013 *Phys. Rev. Lett.* **111** 209601
[41] Yunker P J, Lohr M A, Still T, Borodin A, Durian D and Yodh A 2013 *Phys. Rev. Lett.* **111** 209602
[42] Dhillon P K and Sarkar S 2013 *Appl. Surf. Sci.* **284** 569–574
[43] Dhillon P K and Sarkar S 2016 *Curr. Appl. Phys.* **16** 956–962
[44] López J M, Rodriguez M A and Cuerno R 1997 *Phys. Rev. E* **56** 3993–3998
[45] Ramasco J J, López J M and Rodriguez M A 2000 *Phys. Rev. Lett.* **84** 2199–2202
[46] Schwarzacher W 2004 *J. Phys.: Condensed Matter* **16** R859–R880
[47] Palik E, Glembocki O, Heard Jr I, Burno P and Tenerz L 1991 *J. Appl. Phys.* **70** 3291–3300
[48] Suárez M, Mirabella D and Aldao C 2008 *J. Mol. Catal. A: Chem.* **281** 230–236
[49] Zhao Y, Wang G C and Lu T M 2001 *Characterization of Amorphous and Crystalline Rough Surface: Principles and Applications* (San Diego: Academic Press)
[50] Pelliccione M and Lu T M 2008 *Evolution of thin film morphology: modeling and simulations* vol 108 (Heidelberg: Springer Science & Business Media)
[51] URL `http://gwyddion.net`
[52] Ruiz R, Nickel B, Koch N, Feldman L C, Haglund R F, Kahn A, Family F and Scoles G 2003 *Phys. Rev. Lett.* **91** 136102
[53] Plischke M and Bergersen B 2006 *Equilibrium statistical physics* (Singapore: World Scientific Publishing)
[54] Oliveira T J and Aarão Reis F D A 2007 *J. Appl. Phys.* **101** 063507
[55] Oliveira T J and Aarão Reis F D A 2011 *Phys. Rev. E* **83** 041608
[56] Vivo E, Nicoli M, Engler M, Michely T, Vázquez L and Cuerno R 2012 *Phys. Rev. B* **86** 245427
[57] Reis F A 2003 *Phys. Rev. E* **68** 041602
[58] Gupta A, Aldinger B S, Faggin M F and Hines M A 2010 *J. Chem. Phys.* **133** 044710
[59] Pietsch G, Higashi G and Chabal Y 1994 *Appl. Phys. Lett.* **64** 3115–3117